IEEE Access
Multidisciplinary | Rapid Review | Open Access Journal

Received August 3, 2018, accepted August 28, 2018, date of publication September 3, 2018, date of current version September 21, 2018.

Digital Object Identifier 10.1109/ACCESS.2018.2868414

A Triple-Band Dual-Polarized Indoor Base Station Antenna for 2G, 3G, 4G and Sub-6 GHz 5G Applications

AHMED ALIELDIN[1], YI HUANG[1], (Senior Member, IEEE), STEPHEN J. BOYES[2], (Member, IEEE), MANOJ STANLEY[1], SUMIN DAVID JOSEPH[1], QIANG HUA[1], AND DAJUN LEI[1]

[1]Department of Electrical Engineering and Electronics, The University of Liverpool, Liverpool L69 3GJ, U.K.
[2]Defence Science and Technology Laboratory, Sevenoaks TN14 7BS, U.K.

Corresponding author: Yi Huang (yi.huang@liverpool.ac.uk)

ABSTRACT This paper proposes a new design of a triple-band dual-polarized indoor base station antenna for mobile communication systems serving the 2G, 3G, 4G, and the new sub-6 GHz 5G applications. The design consists of two orthogonal dipole antennas to provide dual polarization. Each dipole consists of three different radiator types—elliptical dipole, bowtie dipole, and cat-ear shaped arms for different bands. The proposed antenna offers three broad bands with the fractional bandwidths of 31.3% (0.7–0.96 GHz), 55.3% (1.7–3 GHz), and 14% (3.3–3.8 GHz) which can be controlled independently. The design also offers stable radiation patterns within the desired frequency bands, high polarization purity and, a simple feeding structure with a compact size and low profile which make this new design an ideal candidate for indoor mobile base stations serving the 2G, 3G, 4G, and the new sub-6GHz 5G applications.

INDEX TERMS Base station antenna, crossed dipoles, dual-polarization antenna, triple-band antenna.

I. INTRODUCTION

As telecommunication vendors look to introduce 5G mobile communication systems from 2019, base station and mobile antennas need to evolve to fulfil the new sub-6 GHz 5G frequency bands in addition to the existing 2G, 3G and 4G bands (0.7-0.96 GHz and 1.7-2.7 GHz). In 2016, the European Commission (EC) announced its spectrum plan for 5G trials covering the bands from 3.4 to 3.8 GHz. In 2017, the Chinese Ministry of Industry and Information Technology (MIIT) officially declared that 3.3-3.4 (indoor only), 3.4 -3.6 and 4.8-5 GHz bands are allocated for 5G services [1]. For base station antennas, diversity in space and/or polarization has been used to improve the signal-to-noise ratio (SNR) and system performance [2]. Base station antennas should maintain good impedance matching within the entire frequency bands of interest, a stable radiation pattern and also a high polarization purity (PP) simultaneously [3]. For indoor base stations where the available spaces to install antennas are limited, it is favorable to have a single antenna element covering the frequency bands of interest rather than multi antennas for multi bands. Many attempts have been done to satisfy the 2G, 3G and 4G applications by a single antenna covering the frequency bands from 0.7 to 0.96 GHz (B1) and from 1.7 to 2.7 GHz (B2). In [4], dual-polarized performance was achieved for both bands (B1 and B2) but the impedance bandwidths (BW) were insufficient (0.86 – 096 GHz for B1 and 1.7-1.9 for B2). In [5], the BWs were improved but only a single polarization was provided which makes the design not suitable for base station applications. There are many other designed. For example, in [6]–[8], BWs were much improved either by using irregular shorted patches as in [6] or dual-band dipoles as in [7] and [8]. Unfortunately, these reported designs again are single polarization. In [9], a dual-band dual-polarized antenna was presented but the BWs are not wide enough for 2G, 3G and, 4G communication systems. Due to the introduction of 5G, single-polarized dual-band indoor base station antennas were reported to cover B2 and the new sub-6 GHz 5G frequency band from 3.3 to 3.8 GHz (B3). In [10], a single-polarized dual-band folded dipole antenna was designed to operate across 2.3-2.5 GHz and 3.1-4.2 GHz. In [11] and [12], single antennas were produced to cover most of the frequencies in B2 and B3 simultaneously, from 1.8 to 3.77 GHz in [11] and from 2.4 to 3.6 GHz in [12]. Recently, an E-shaped triple-band patch antenna was presented in [13]

to cover B1, B2 and B3 simultaneously. The main drawbacks of this design are that the BWs are not sufficient (0.92-0.96 GHz, 1.9-2.2 GHz and, 3.4-3.8 GHz) and it is single polarization.

This paper proposes a novel design of a dual-polarized triple-band antenna for 2G, 3G, 4G and, sub-6 GHz 5G indoor base stations covering the frequency bands from 0.7-0.96 GHz, 1.7-2.7 GHz and, 3.3-3.8 GHz simultaneously. The design consists of two cross dipoles. Each dipole may be considered as a combination of three different types of radiator (typically one type for each band); elliptical dipole (type 1), bowtie dipole (type 2) and cat-ear shaped arms (type 3). As each radiator parameters can be controlled individually, the three bands (B1, B2 and, B3) can be tuned independently to achieve excellent triple broad performance.

The paper is organized as follows: Section II describes the proposed antenna configuration and its principle of operations, Section III discusses its performance and a sensitive study of its parameters and finally, conclusions are presented in Section IV.

II. THE PROPOSED ANTENNA DESIGN

A. ANTENNA CONFIGURATION

Fig. 1 illustrates the geometry of the proposed antenna. Generally, we can describe the geometry as a pair of two orthogonal crossed dipoles: dipole A and dipole B. Dipole A consists of an elliptical-shaped dipole (type 1) placed on 45° with respect to Y-axis. The two elliptical arms of dipole A are printed on opposite sides of an FR-4 substrate with relative permittivity $\varepsilon_r = 4.3$, tangential loss of 0.025, thickness of 1.6 mm and side length *Ld*. The two arms are fed through a strip (printed on the substrate top layer) and a 50 Ω coaxial cable. For practical implementation, a hole in the bottom arm is drilled to insert the 50 Ω coaxial feed. The endpoints of the elliptical dipole are extended to form a bowtie dipole (type 2) which is placed orthogonally to the ellipse major axis. Furthermore, a pair of cat-ears (type 3) are added to each elliptical arm such that the major axes of the two cat-ears are intersecting at the ellipse center and forming angles of ±45° with the ellipse major axis respectively. So, in summary, we can describe dipole A as a combination of three different types of radiators; type 1: elliptical dipole, type 2: bowtie dipole and, type 3: cat-ear arms.

The second crossed dipole (dipole B) is a rotated replica of dipole A with a relative angle of 90° around Z-axis. There are two major differences between dipoles A and B. The first difference is that the feeding strip of dipole B is modified. One part of the strip is printed on the bottom layer of the substrate, and then is connected to the top parts through two vias to avoid intersecting with the feeding strip of dipole A. Each via is fabricated by first drilling a hole through the FR-4 substrate, then drawing a copper wire through the hole, and finally by soldering the copper wire to the strip line on both sides of the substrate. The second major difference is that one of the cat-ears in the bottom layer is shifted to the top layer to add a capacitive loading to the input impedance (Zin)

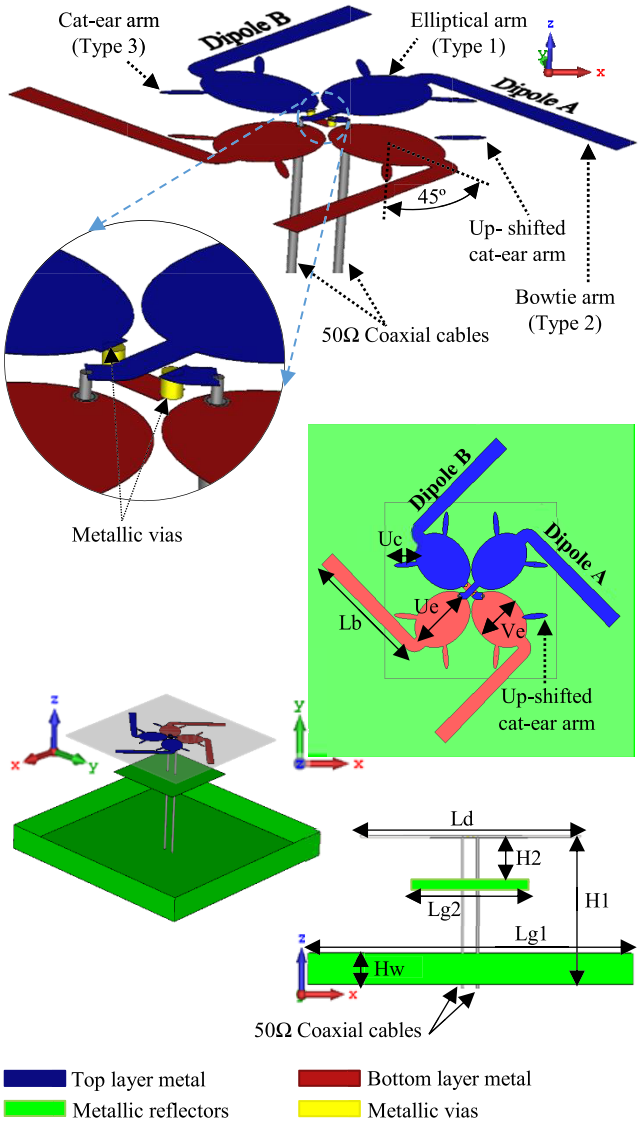

FIGURE 1. The geometry of the proposed antenna.

of dipole B to compensate the inductive effect introduced by the vias as discussed in detail in the next section. Thus, the distribution of the cat-ears at dipole B is asymmetric (three on the top layer and one on the bottom layer) unlike their symmetric distribution at dipole A (two on each side). The substrate and dipoles are oriented in the XY plane as shown in Fig. 1. The substrate is placed above two square metallic ground reflectors to enable directional radiation, a large reflector for the lower frequencies band B1 and a small reflector for the higher frequencies bands B2 and B3. The large reflector is placed at a height of H1 from the substrate, with a side length Lg1 and four sidewalls of a height of Hw while the small reflector is placed at a height of H2 from the substrate and has a side length Lg2. The substrate and the two metallic reflectors are concentric and their edges are parallel to X and Y-axes. The optimized dimensions are determined as follows (in mm): $Ue = 29$, $Ve = 21.4$, $Lb = 54$, $Uc = 11.6$,

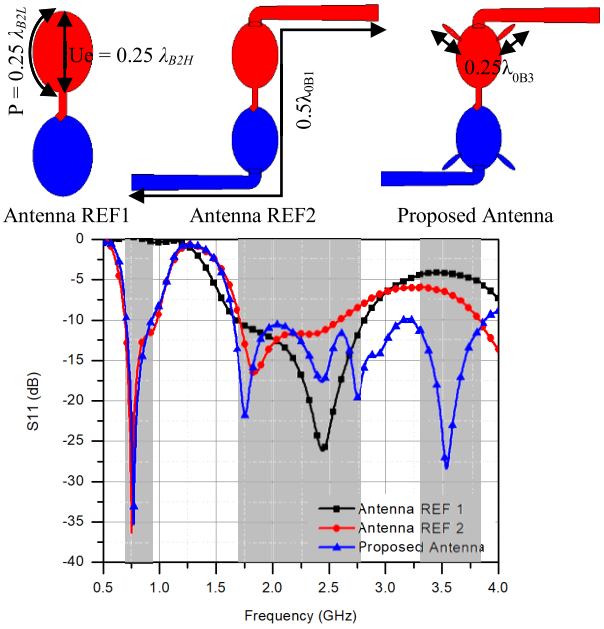

FIGURE 2. References and the proposed antenna designs.

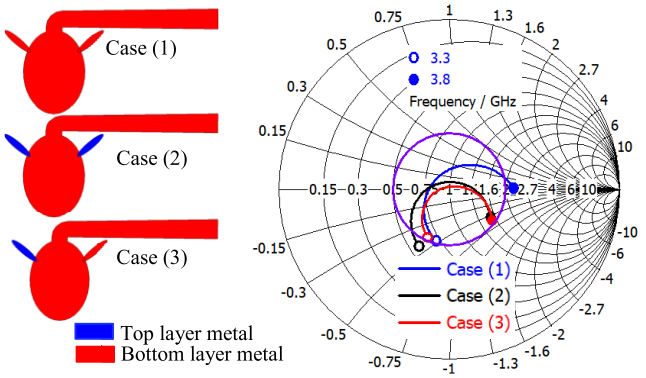

FIGURE 3. Effect of the cat-ear arm position on Zin of dipole B across B3.

Ld =150, $H1$ = 100, $H2$ = 30; Hw = 23, $Lg1$ = 220 and, $Lg2$ = 80.

B. ANTENNA PRINCIPLES OF OPERATION

Two reference designs (antenna Ref 1 and antenna Ref 2) can be employed to understand the working principle of the proposed design as shown in Fig. 2. Initially, antenna Ref 1 was designed based on the elliptical dipole (type 1) to cover B2 as it has the widest BW among the three desired bands [14]. The ellipse major and minor axes (Ue and Ve) are selected such that the shortest current path length from the feeding point to the end point of the ellipse (Ue) equals to $0.25\lambda_{B2H}$ while the longest current path length from the feeding point to the end point of the ellipse (P) equals to $0.25\lambda_{B2L}$ (where λ_{B2H} and λ_{B2L} are the free space wavelength at the highest and lowest frequencies of B2 respectively and P is half of the ellipse circumference). P is related to the axes lengths as:

$$P = \pi\sqrt{\frac{\left(\frac{Ue}{2}\right)^2 + \left(\frac{Ve}{2}\right)^2}{2}} = \frac{\lambda_{B2L}}{4} \quad (1)$$

It is worth noting that all current path lengths from the feeding point to the ellipse end point ranging from the shortest path Ue to the longest path P are equal to a quarter of the wavelengths ranging from λ_{B2H} to λ_{B2L} respectively. Thus, the dipole length may be considered as a half wavelength for the all the frequencies within B2.

In antenna Ref 2, a bowtie dipole with a total length of $2Lb$ (type 2) is combined with the elliptical dipole. Each arm of the bowtie dipole is connected to one of the endpoints of the elliptical dipole and forming 90° with respect to the ellipse major axis. The dimension Lb was initially selected such that the dipoles total length ($2Ue+2Lb$) equals to $0.5\lambda_{0B1}$ (where λ_{0B1} is the free space wavelength of the central frequency of B1 0.83 GHz). Thus, B1 and B2 are fully covered by a combinational design of type 1 and type 2.

Furthermore, in the proposed design, the cat-ear arms (type 3) are combined to the antenna Ref 2. The major axes of the cat-ear arms form angles of ±45° with the ellipse major axis respectively. Thus, each pair lies on one of two perpendicular axes (X-axis and Y-axis). The dimension Uc was initially selected such that the total length of each pair of cat-ear arms ($2Uc$) is $0.25\lambda_{0B3}$ (where λ_{0B3} is the free space wavelength of the central frequency of B3 3.55 GHz). So, the triple-band performance is achieved.

As mentioned in the previous section, in dipole B (which has two vias through the feeding strip), one of the cat-ear arms should be shifted from the bottom layer to the top layer to create a capacitive loading and compensate the inductive effect of the vias. For better understanding of this matter, Fig. 3 shows three cases of different positions of the cat-ear arms at dipole B. Case (1) is the initial case where both cat-ear arms are in the bottom layer of the substrate. So, B3 is not fully covered with VSWR ≤ 2 (the fully complete (purple) circle in the middle of the Smith chart) due to the inductive effect of the vias especially at the stop frequency of B3 (note that the higher the frequency, the more sensitive Zin to any inductance change). In case (2), both cat-ear arms are shifted to the top layer of the substrate to add two parallel capacitive loadings between them and the elliptical arm. Thus, Zin across B3 becomes too capacitive especially at the start frequency of B3 (note that the lower the frequency, the more sensitive Zin to any capacitive change). Case (3) is the proposed design where one of the cat-ear arms is printed on the bottom layer while the other is shifted to the top layer. In this case, B3 is fully covered with VSWR ≤ 2. It is worth noting that the vias do not have any significant effect on the impedance matching across B1 and B2 as their reactance is too small at these bands.

Fig 4 shows the current distribution across the dipole at the central frequency of each band. It can be seen that at B1, the current flows from the feeding point to the terminal points through bowtie and elliptical dipoles which indicates that

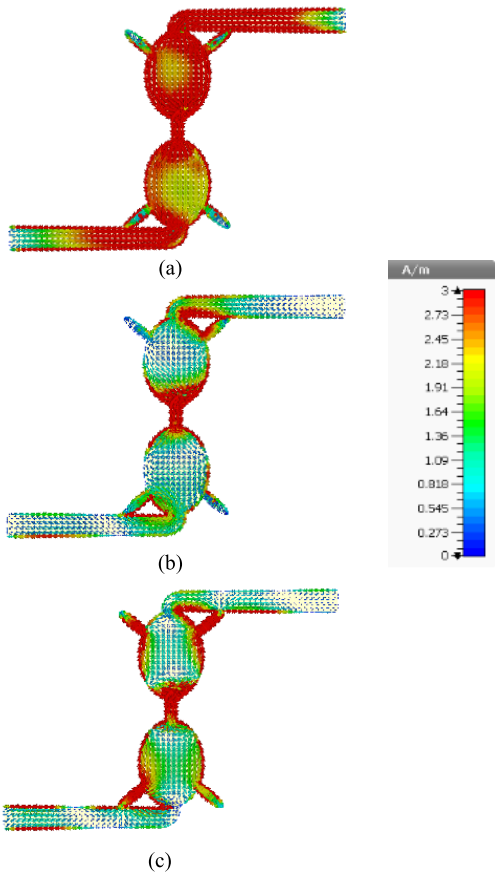

FIGURE 4. The current distributions at the central frequency of (a) B1 (b) B2 (c) B3.

TABLE 1. Contributions of the three radiator types to the radiation.

Frequency Band	Radiator Type		
	Type 1 (Elliptical)	Type 2 (Bowtie)	Type 3 (Cat-ears)
B1	✓	✓	
B2	✓		
B3			✓

these two radiator types (1 and 2) are the radiators across B1. On the other hand, the current distribution at B2 is highly dense around the elliptical dipole while there is a small current density across the bowtie and cat-ears. Furthermore, at B3, the current density is high at the cat-ears with small current density across the elliptical and bowtie dipoles.

Table 1 summaries the contributions of each type of the three radiator types to the radiation across each band. It is evident from table 1 that B1 and B3 can be tuned independently by controlling the dimensions of the bowtie and cat-ears respectively. More illustrations will be presented in the next section.

III. THE PROPOSED ANTENNA RESULTS

To validate the proposed design, a prototype was fabricated and tested as shown in Fig. 5. The simulation was accomplished by using CST microwave studio. Measured results

TABLE 2. The HPBWs, PP and gains of the proposed antenna.

Frequency Band	HPBW (°)		PP (dB)	Average Gain (dBi)
	H-Plane	V-Plane		
B1	73±2	100±5	≥ 20	5.5
B2	65±5	72±8	≥ 18	8
B3	80±6	70±8	≥ 15	5.5

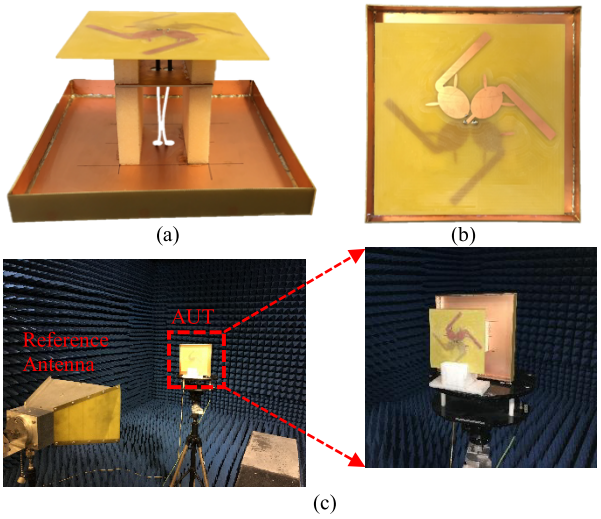

FIGURE 5. A prototype of the proposed antenna (a) side view (b) top view (c) during measurements.

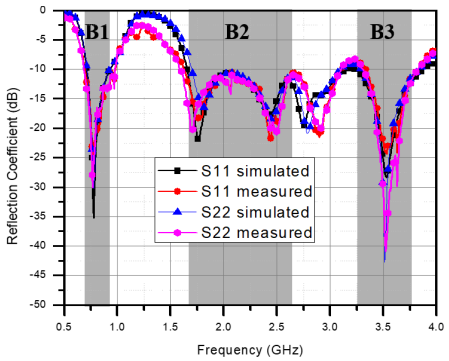

FIGURE 6. Simulated and measured reflection coefficients.

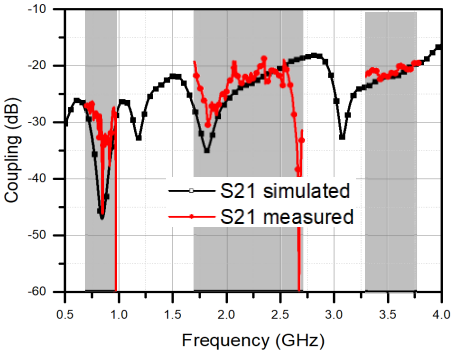

FIGURE 7. Simulated and measured port-to-port isolations.

of S-parameters, gain, and radiation patterns were obtained by using a Vector Network Analyzer (VNA) and an anechoic chamber.

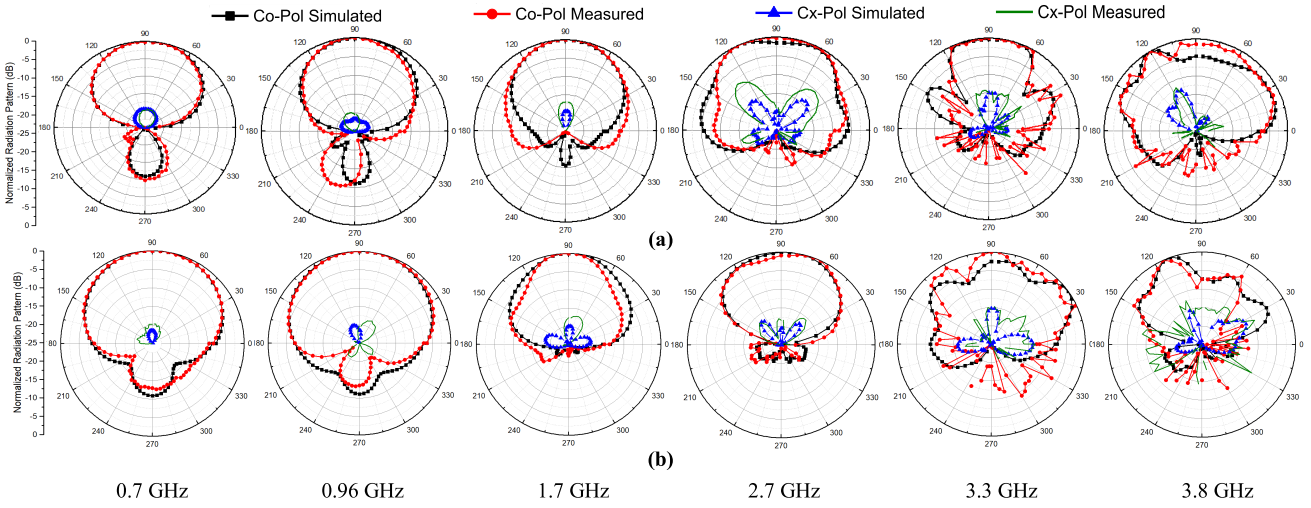

FIGURE 8. Simulated and measured co- and cross-polarized radiation patterns in (a) H-plane (b) V-plane.

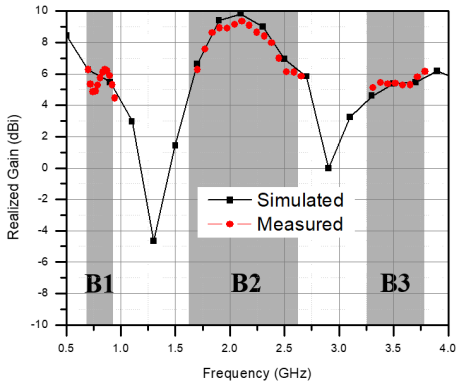

FIGURE 9. The proposed antenna simulated and measured realized gains.

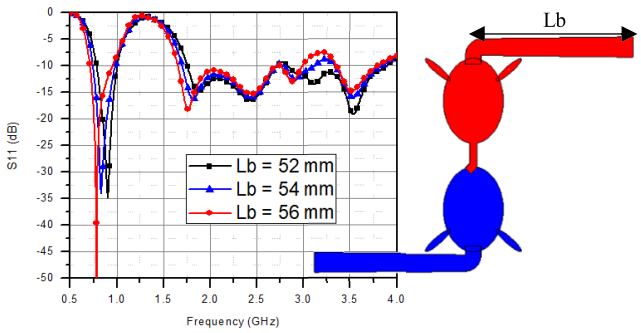

FIGURE 10. Effect of Lb on the reflection coefficient.

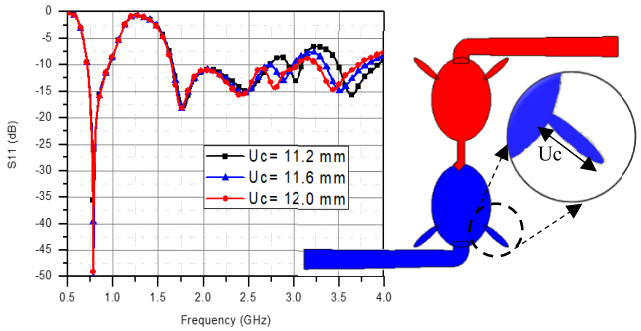

FIGURE 11. Effect of Uc on the reflection coefficient.

Fig. 6 shows a good agreement between the simulated and measured reflection coefficients for both ports. For VSWR ≤ 2, the fractional BWs are 31.3% (0.7-0.96 GHz), 55.3% (1.7 -3 GHz) and, 14% (3.3-3.8 GHz) for B1, B2 and, B3 respectively. Fig. 7 shows that the measured port-to-port isolation is better than 27 dB for B1 which meets the general criteria for base station antennas (typically 25 dB) [15]. For B2 and B3, isolations are better than 20 dB which ideally should be more than 25 dB (thus this is a possible drawback of this design). This happens because of the high surface current density formed at the feed point at B2 and B3 (see Fig. 4).

The simulated and measured co- and cross-polarized radiation patterns at the start and stop frequencies of each band in H-plane (XZ plane) and V-plane (YZ plane) are shown in Fig. 8. It is apparent that the proposed antenna has a good agreement in radiation pattern between the simulations and the measurements. The radiation patterns may have some distortions at B3. These distortions are due to the large substrate aperture in terms of λ_{0B3} ($2\lambda_{0B3} \times 2\lambda_{0B3}$). But, radiation patterns are still applicable for indoor base station antenna usage across the three bands. The HPBWs and the PP are illustrated in Table 2. Fig. 9 presents the proposed antenna realized gains at B1, B2 and, B3 in simulation and measurements.

The antenna has a stable gain across the entire bands. The average realized gains are tabulated in Table 2. Table 3 displays a comparison between multi-band indoor base station antennas performance and the proposed antenna.

For a fair comparison, the size of each antenna is normalized to λ_L (where λ_L is the wavelength at the lowest operating frequency). It is apparent that the proposed antenna

TABLE 3. Comparison of several multi-band antennas to the proposed antenna.

Ref		[4]	[5]	[6]	[7]	[8]	[9]	[10]	[11]	[12]	[13]	This Work
Fractional BW (%)	B1	11%	26.7%	34%	17.5%	28.6%	14.1%	-	-	-	4.3%	**31.3%**
	B2	11.1%	44%	35.4%	21.2% - 33%	11.1%	24.7%	8.3%	36.1%	11%	14.6%	**55.3%**
	B3	-	-	-	-	-	-	29%	36.1%	11%	11.1%	**14.1%**
HPBW (°)	B1	NA	60	103	360	80	63	-	-	-	40	**73**
	B2	NA	40	57	360	60	85	60	360	66	60	**65**
	B3	-	-	-	-	-	-	60	360	49	120	**80**
Average Gain (dBi)	B1	6.5	8.4	7	2	6	11.8	-	-	-	NA	**5.5**
	B2	7.3	8	8	2	9	7	9	2.9	9.2	NA	**8**
	B3	-	-	-	-	-	-	9	5.5	7	NA	**5.5**
PP (dB)	B1	18	12	26	NA	NA	NA	-	-	-	NA	**20**
	B2	30	15	28	NA	NA	NA	40	NA	19	NA	**18**
	B3	-	-	-	-	-	-	29	NA	19	NA	**15**
Front-to-Back lobe ratio (dB)	B1	NA	-18	18	NA	12	21.2	-	-	-	NA	**10**
	B2	NA	-18	20	NA	18	4.1	22	NA	14	NA	**15**
	B3	-	-	-	-	-	-	22	NA	14	NA	**18**
Polarization		Dual	Single	Single	Single	Single	Dual	Single	Single	Single	Single	**Dual**
Antenna Size(λ_L)		0.3×0.3 ×.04	0.33×0.33 ×0.2	0.48×0.28 ×0.12	0.3×0.04 ×0.005	0.6×0.15 ×0.6	0.68×0.51 ×0.06	0.6×0.4 ×0.25	0.6×0.3 ×0.005	0. 5×0.25 ×0.1	0.3×0.2 ×0.03	**0.35×0.35 ×0.23**

can operate across the three bands simultaneously with broad BWs and dual-polarized performance. It also has a relatively small size. Note that the reported omnidirectional base station antennas in [7] and [11] have low profiles as they do not have reflectors.

As mentioned in the previous section, B1 and B3 can be tuned independently by controlling the parameters of the bowtie and cat-ear radiators (types 2 and 3) respectively. So, to optimize the proposed antenna BW, it is necessary to understand how these parameters affect the antenna performance. Their effects are studied through simulations.

A. EFFECT OF THE BOWTIE DIPOLE LENGTH (TYPE 2)

The first parameter to be studied is the bowtie arm length (*Lb*). As has been stated in Table 1, the bowtie dipoles contribute to the radiation across B1 only with a very slight effect on B2 and B3. Thus, B1 can be controlled independently from B2 and B3 by changing the length Lb. As noticed in Fig. 10, when the length *Lb* increases, B1 is shifted to lower frequencies while B2 has almost no changes. It has slight changes in B3 due to the coupling between the bowtie arm and the closest cat-ear arm. Anyway, there is almost no change in the BW across B3 due to this coupling. The optimum value of *Lb* is found to be 54 mm to cover the whole B1 with VSWR ≤ 2.

B. EFFECT OF THE CAT-EAR ARM LENGTH (TYPE 3)

The second parameter to be studied is the cat-ear arm length *Uc*. Changing *Uc* does not result in any changes in B1 and B2. Thus, B3 can be tuned by changing the dimension *Uc* as shown in Fig. 11. The optimum value of *Uc* is found to be 11.6 mm to fully cover B3.

IV. CONCLUSION

A novel triple-band dual-polarized antenna for mobile indoor base station has been designed, optimized, fabricated and measured. It covers the frequency bands from 0.7 to 0.96 GHz, from 1.7 to 3 GHz and, from 3.3 to 3.8 GHz simultaneously with high PP. The proposed antenna consists of a combination of three different types of radiators. Typically one type for each band. The multiband performance is achieved by optimizing each type which is associated to each band independently. Because of its multiband performance, its dual polarization capabilities and small size, the proposed antenna is an excellent candidate for mobile indoor base station which operates over the new sub-6 GHz 5G applications in addition to the exciting 2G, 3G and, 4G applications.

REFERENCES

[1] Q. Wu, P. Liang, and X. Chen, "A broadband ±45° dual-polarized multiple-input multiple-output antenna for 5G base stations with extra decoupling elements," *J. Commun. Inf. Netw.*, vol. 3, no. 1, pp. 31–37, Mar. 2018.

[2] X.-P. Mao and J. W. Mark, "On polarization diversity in mobile communications," in *Proc. Int. Conf. Commun. Technol.*, Guilin, China, Nov. 2006, pp. 1–4.

[3] Q.-X. Chu, Y. Luo, and D.-L. Wen, "Three principles of designing base-station antennas," in *Proc. Int. Symp. Antennas Propag. (ISAP)*, Hobart, TAS, Australia, Nov. 2015, pp. 1–3 2015.

[4] T.-W. Chiou and K.-L. Wong, "A compact dual-band dual-polarized patch antenna for 900/1800-MHz cellular systems," *IEEE Trans. Antennas Propag.*, vol. 51, no. 8, pp. 1936–1940, Aug. 2003.

[5] P. Li, K. M. Luk, and K. L. Lau, "A dual-feed dual-band L-probe patch antenna," *IEEE Trans. Antennas Propag.*, vol. 53, no. 7, pp. 2321–2323, Jul. 2005.

[6] W. X. An, H. Wong, K. L. Lau, S. F. Li, and Q. Xue, "Design of broadband dual-band dipole for base station antenna," *IEEE Trans. Antennas Propag.*, vol. 60, no. 3, pp. 1592–1595, Mar. 2012.

[7] Iswandi, A. K. D. Jaya, and E. S. Rahayu, "Design of triple band printed dipole antenna for indoor small cell base station in LTE systems," in *Proc. 2nd Int. Conf. Inf. Technol., Inf. Syst. Elect. Eng. (ICITISEE)*, Yogyakarta, Indonesia, Nov. 2017, pp. 207–210.

[8] A. Edalati and W. McCollough, "A novel dual-band beam-switching antenna based on active frequency selective surfaces," in *Proc. IEEE Int. Symp. Antennas Propag. USNC/URSI Nat. Radio Sci. Meeting*, San Diego, CA, USA, Jul. 2017, pp. 1985–1986.

[9] S. Nikmehr and K. Moradi, "Design and simulation of triple band GSM900/DCS1800/UMTS2100 MHz microstrip antenna for base station," in *Proc. IEEE Int. Conf. Commun. Syst.*, Singapore, Nov. 2010, pp. 113–116.

[10] Z. Wang, G.-X. Zhang, Y. Yin, and J. Wu, "Design of a dual-band high-gain antenna array for WLAN and WiMAX base station," *IEEE Antennas Wireless Propag. Lett.*, vol. 13, pp. 1721–1724, 2014.
[11] A. Toktas and A. Akdagli, "Wideband MIMO antenna with enhanced isolation for LTE, WiMAX and WLAN mobile handsets," *Electron. Lett.*, vol. 50, no. 10, pp. 723–724, May 2014.
[12] M. van Rooyen, J. W. Odendaal, and J. Joubert, "High-gain directional antenna for WLAN and WiMAX applications," *IEEE Antennas Wireless Propag. Lett.*, vol. 16, pp. 286–289, 2017.
[13] K. Yu, Y. Li, X. Luo, and X. Liu, "A modified E-shaped triple-band patch antenna for LTE communication applications," in *Proc. IEEE Int. Symp. Antennas Propag. (APSURSI)*, Fajardo, Puerto Rico, Jun./Jul. 2016, pp. 295–296.
[14] A. Alieldin and Y. Huang, "Design of broadband dual-polarized oval-shaped base station antennas for mobile systems," in *Proc. IEEE Int. Symp. Antennas Propag. USNC/URSI Nat. Radio Sci. Meeting*, San Diego, CA, USA, Jul. 2017, pp. 183–184.
[15] C. Ding, H. Sun, R. W. Ziolkowski, and Y. J. Guo, "Simplified tightly-coupled cross-dipole arrangement for base station applications," *IEEE Access*, vol. 5, pp. 27491–27503, 2017.

AHMED ALIELDIN received the B.Sc. degree in radar engineering from the Military Technical College, Egypt, in 2005, and the M.Sc. (Eng.) degree in antenna and microwave propagation from the University of Alexandria, Egypt, in 2013. He is currently pursuing the Ph.D. degree in electrical engineering with The University of Liverpool, U.K. He was a Radar Engineer under MoD, Egypt, and a Lecturer Assistant with the Air Defence College, Egypt. He was an Antenna Engineer with Benha Electronics Company, where he was involved in projects of national importance. His research interests include mobile base station antennas, satellite antennas, MIMO, and phased-MIMO radar antenna arrays design.

YI HUANG (S'93–A'95–M'96–SM'06) received the B.Sc. degree in physics and the M.Sc. (Eng.) degree in microwave engineering Wuhan University, Wuhan, China, and the D.Phil. degree in communications from the University of Oxford, Oxford, U.K., in 1994.

He was a Radar Engineer with NRIET, Nanjing, China, and various periods with the Universities of Birmingham, Birmingham, U.K., Oxford and Essex as a Research Staff Member. In 1994, he joined as a Research Fellow at British Telecom Labs, London, U.K., and then joined the Department of Electrical Engineering and Electronics, The University of Liverpool, as a Lecturer, in 1995, where he is currently a Chair in wireless engineering with the Deputy Head of Department, the Head of High-Frequency Engineering Research Group, and the M.Sc. Program Director. He has authored over 300 refereed papers in leading international journals and conference proceedings and books on *Antennas: From Theory to Practice* (John Wiley, 2008) and *Reverberation Chambers* (Wiley, 2016). His current research interests include radio communications, applied electromagnetics, radar, and antennas since 1987.

Dr. Huang has received many research grants from research councils, government agencies, charity, EU, and industry, acted as a consultant to various companies, and served on a number of the National and international technical committees, such as the IET, EPSRC, European ACE, COST-IC0603, and COST-IC1102, and EurAAP. He has been an editor, an associate editor, or a guest editor of four of international journals. He has been a Keynote/Invited Speaker and Organizer of many conferences and workshops, such as the IEEE iWAT, WiCom, and LAPC. He is fellow of the IET. He is currently the Editor-in-Chief of *Wireless Engineering and Technology* (ISSN 2152-2294/2152-2308), an Associate Editor of the IEEE Antennas and Wireless Propagation Letters, a College Member of EPSRC, U.K./Ireland Delegate to EurAAP.

STEPHEN J. BOYES received B.Eng. degree (Hons) in electronic and communication engineering, the M.Sc. (Eng.) degree in microelectronic systems and telecommunications, and the Ph.D. degree in antennas/electromagnetics from The University of Liverpool.

His academic research activities and Ph.D. at The University of Liverpool was centered on reverberation chambers, with an emphasis on a wide variety of antennas and antenna measurements for communication applications. His academic research work covered novel textile antennas, multiple-input multiple-output (MIMO) antennas and novel antenna arrays.

In addition to work in academia, he has also held various posts throughout 10 years working in industry. In 2013, he joined the Defence Science and Technology Laboratory, where he is currently a Senior RF Research Scientist leading all antennas and electromagnetics research activities within his group. His present research interests and activities are associated with novel antennas for military applications which include body worn and vehicle borne types. He also leads research into novel frequency selective surfaces, bespoke network configurations and measurements with reverberation chambers and holds numerous patents in the RF field.

He is the main author of a technical book on reverberation chambers published by John Wiley & Sons in 2016 and has also published many papers in leading international journals and conferences. He serves as a technical reviewer for leading academic journals in the antennas and propagation field as well as sitting on major International committees on behalf of the U.K, chairing one such technical committee on novel antenna design.

MANOJ STANLEY received the B.Tech. degree in electronics and communication from Kerala University, India, in 2012, and the M.Tech. degree in communication systems from the Visvesvaraya National Institute of Technology, India, in 2014. He is currently pursuing the Ph.D. degree in electrical engineering with The University of Liverpool, U.K. He was a Lab Engineer under CoE with the Visvesvaraya National Institute of Technology, where he was involved in projects of national importance. His research interests include mobile phone antenna design, theory of characteristic modes, MIMO, and mm-wave antenna array design for 5G smartphones.

SUMIN DAVID JOSEPH received the B.Tech. degree (Hons.) in electronics and communication from the Cochin University of Science and Technology, India, in 2012, the M.Tech. degree (Hons.) in communication systems from the Visvesvaraya National Institute of Technology, India, in 2015. He is currently pursuing the dual Ph.D. degree in electrical engineering with The University of Liverpool, U.K., and National Tsing Hua University, Taiwan.

He was a Lab Engineer under CoE with the Visvesvaraya National Institute of Technology, India, where he was involved in projects of national importance. His research interests include self-biased circulators, mm-wave antenna arrays, rectifying antennas, rectifiers, wireless power transfer, and energy harvesting.

QIANG HUA received the B.Sc. degree in communication engineering from The University of Liverpool, Liverpool, U.K, in 2016, and the M.Sc. degree in digital signal processing from The University of Manchester, Manchester, U.K, in 2017. He is currently pursuing the Ph.D. degree in base station antennas with The University of Liverpool, Liverpool, U.K.

His current research focuses on the base station antenna design for 5G in wireless communications.

DAJUN LEI received the B.S. degree from Hunan Normal University in 1996 and the Ph.D. degree from Hunan University, Changsha, China, in 2011. He is currently a Professor with the School of Electronic Information and Electrical Engineering, Xiangnan University, Chenzhou. He also holds visiting position at the Department of Electrical Engineering and Electronics, The University of Liverpool, U.K.

His research interests are mainly in the fields of dielectric resonator microwave components and planar antennas and arrays.